Research article

Effects of annealing on structural, optical and electrical properties of WO$_3$ films deposited by Sol-Gel Technique

Z. Khalifa, M. Aly and A. A. Aboud

Department of Physics, Faculty of Science, Beni Suef University, Egypt

E-mail: co3o42000@yahoo.com

Abstract

 In this study, deposition of tungsten trioxide (WO$_3$) thin films on fused silica substrates has been performed by sol-gel technique using precursor based on non-alkoxide materials. Preparation of peroxotungstic acid (PTA) precursor of enhanced stability has been carried out by dissolving tungsten metal in excess hydrogen peroxide under controlled temperature. WO$_3$ thin films have been deposited on fused silica substrates by spin coating technique using air blowed solution of PTA. X-ray diffraction investigations showed that the as-deposited films dried at 120°C are amorphous. Annealing the as-deposited film at temperature of 500˚C for 2 hours in air gave the monoclinic form of WO$_3$ with preferred orientation along the (200) direction. Scanning electron microscope photographs showed that the film annealed at 500˚C has a uniform surface morphology. The direct allowed energy gap (E$_g$) of the annealed films of WO$_3$ has been found to lie in the range ~ 2.9-3.7 eV depending on the annealing temperature. The activation energy values for electrical conduction have been found to depend strongly on the crystallinity of the films.

Keywords : Tungsten trioxide; sol-gel technique; thin films.

1. Introduction

Tungsten trioxide (WO_3) is one of the transition metal oxides which have several interesting optical and electrical properties. It is reported that WO_3 has interesting physical properties which make it suitable for a variety of thin and thick film applications including electrochromic devices (1), photochromic materials (2), gasochromic switches [3,4],efficient photolysis (3), selective catalysts (4), and gas sensors [7-11]. Tungsten trioxide thin films have been deposited by several techniques such as thermal evaporation (5), sputtering (6), spray pyrolsis [12,13], electrochemical methods (7) and sol-gel technique [2,4]. Various advantages such as , cost effectiveness, energy saving, deposition of high quality films on large areas are offered by Sol-Gel technique. Moreover, easy and precise control of the microstructure and the water content of the deposited films can be achieved (8). Tungsten alkoxides as precursors, have been used for deposition of WO_3 films (9). But tungsten alkoxides are expensive. To avoid its high costs, nonalkoxide materials are used instead [4, 17-19]. One such nonalkoxide solution for coating WO_3 thin films based on the peroxotungstic acid has been reported by Agnihotry et al. (10). The solution has been modified by the addition of some organic compounds to deposit WO_3 films [21-23]. In this regard we carry out this study to elucidate some of the rules that govern the structure, microstructure, optical and electrical properties of WO_3 thin films deposited by nonalkoxide solution based on peroxotungstic acid.

2. Experimental details

2.1. Preparation of the gel.

Tungsten metal of purity 99.999% (Aldrich) has been dissolved in excess hydrogen peroxide 30% (Merk). The reaction of tungsten with hydrogen peroxide is exothermic, so the temperature of the container has been maintained at $0^{o}C$ during the reaction. The tungsten metal powder has been dissolved after few hours. Sometimes the reaction is vigorous and accompanied by the formation of a milky solution at a high temperature. Rising of white vapors has been observed during the reaction. The obtained solution has been filtered to remove insoluble matter. Filtration has been repeated a few times till clear colorless solution has been obtained. This solution has been heated in a thermostated water bath maintained at 60 ˚C to remove excess H_2O_2. The heating time at this stage controls the properties of the obtained gel. The solution has been cooled down to room temperature and air blowing technique has been employed overnight till a glassy gel of peroxotungstic acid (PTA) has been obtained.

2.2. Preparation of the sol.

The precursor solutions for depositing films on fused silica substrates have been made by dissolving known concentration of PTA in deionized water.

2.3. Preparation of thin films

A homemade spin coating unit has been used to deposit the films at 4000 rpm for 1 minute. After that the films have been dried at 120˚C for 1 hour, and then annealed at 300, 500 and 700˚C for 2 hours in air.

2.4. Measurement techniques

X-ray diffraction studies (XRD) of the thin films have been recorded in the range of 2θ =10-80˚ by XSPEX x-ray diffractometer with search - match operation version 5.45 copyright 1990-1999, using CoKα radiation with iron filter. The wavelength of the x-rays is 1.79A˚. The d-values have been calculated using XSPEX soft ware. The morphology of the surfaces has been examined by SEM (Jeol JSM-35) with accelerating voltage up to 40 KV and resolution of 50A˚. Each film has been prepared for grain observation by coating the surface with an approximately 10 nm layer of gold. For film thickness measurements, cross-section photographs have been taken to each film. The optical transmittance of the as deposited and annealed thin films have been carried out in the wavelength range 200-800 nm using Shimadzu UV-3101PC scanning double beam spectrophotometer. The sheet resistance has been measured using the conventional two probe method. Two silver paste electrodes 1.3 cm length and 1.8 cm apart has been painted on the WO_3 thin film. The resistance through the film, has been measured using a conventional digital multimeter model GDM-354A. Electrically heated furnace with Ni-NiCr thermocouple has been used to measure the temperature dependence of the electrical conductivity of annealed WO_3 films.
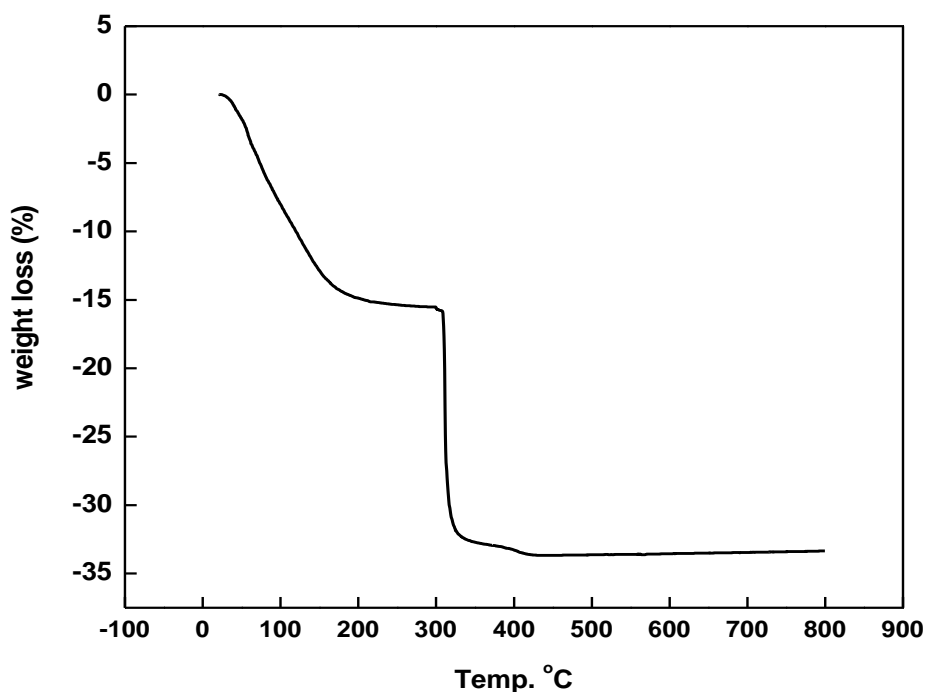
Figure 1: Thermogravimetric analysis (TGA) thermogram for the peroxotungestic acid (PTA) gel

3

3. Results and discussions
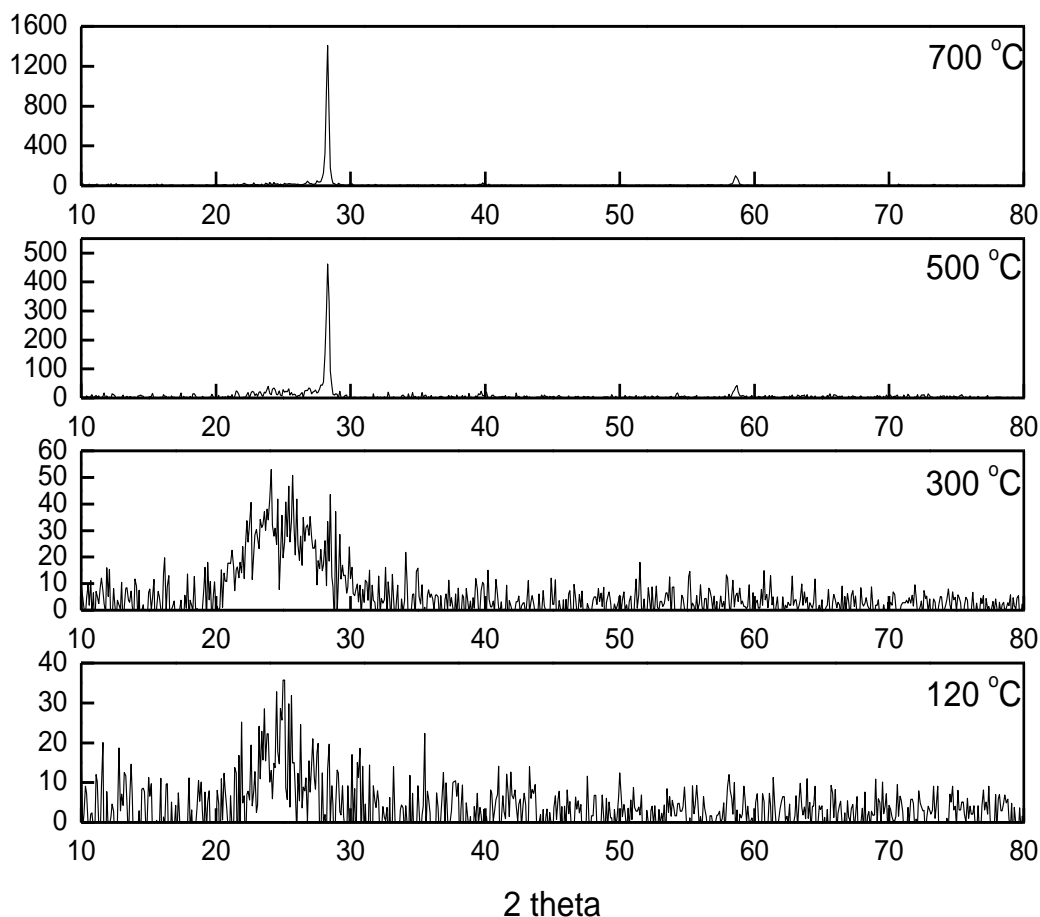
Figure 2: X-ray diffraction patterns of WO_3 thin films annealed for 2 hours at different temperatures.

3.1 Thermal analysis of the PTA gel

The thermal behaviors of the obtained gel have been investigated by thermogravimetric analysis (TGA). The TGA result is shown in Figure 1. Gradual weight loss could be observed in the temperature range 21-200°C. This loss could be attributed to drying of the used sample. After that weight stability is observed up to temperature of 300°C. This second weight loss could be caused by the decomposition of residual chemicals or by the formation of some crystallites.

3.2 X-ray diffraction and microstructure study

4

X-ray diffraction (XRD) patterns of dried and annealed layers are shown in **Error! Reference source not found.**. Dried film shows a broad hump at low 2θ values between 4-35° which is a characteristic feature of a short range order relevant to amorphous phase of the material of this film. This amorphous nature still exists up to annealing temperature 300°C. After that and at 500°C, a big significant peak appeared at 2θ = 28.35^o corresponding to d-value = 3.6611Å (11) with preferred orientation along (200) direction. The XRD pattern for the sample annealed at 700°C revealed a complete crystallization of the film material in the same direction.
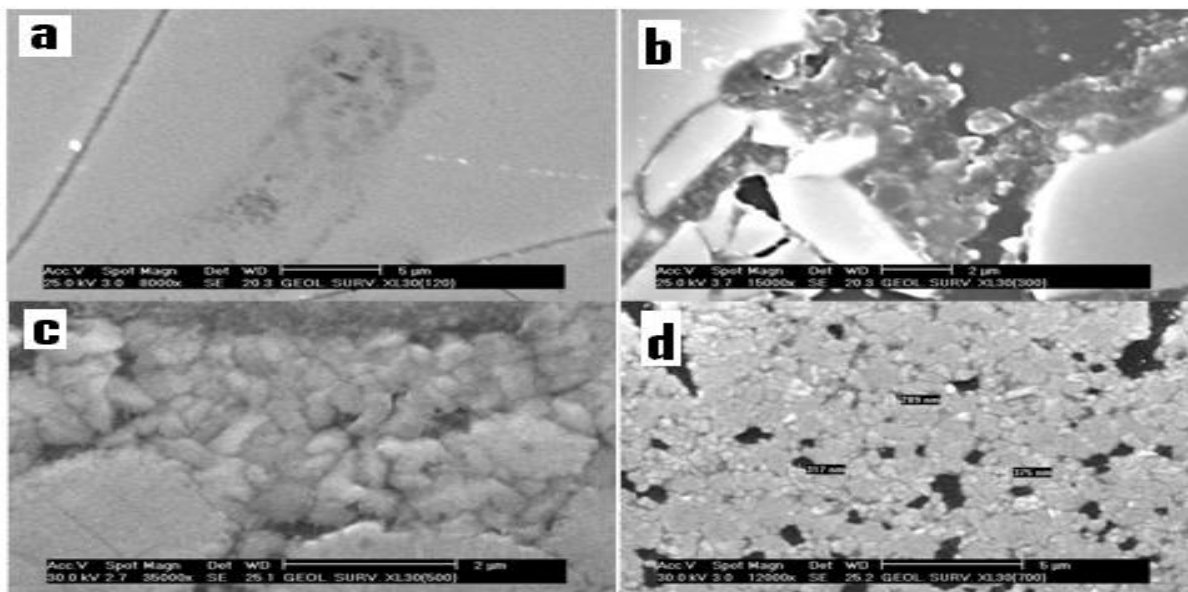
Figure 3: SEM micrographs for films a) dried at 120°C, b) annealed at 300°C for 2 hours, c) annealed at 500°C for 2 hours , and d) annealed at 700°C for 2 hours.
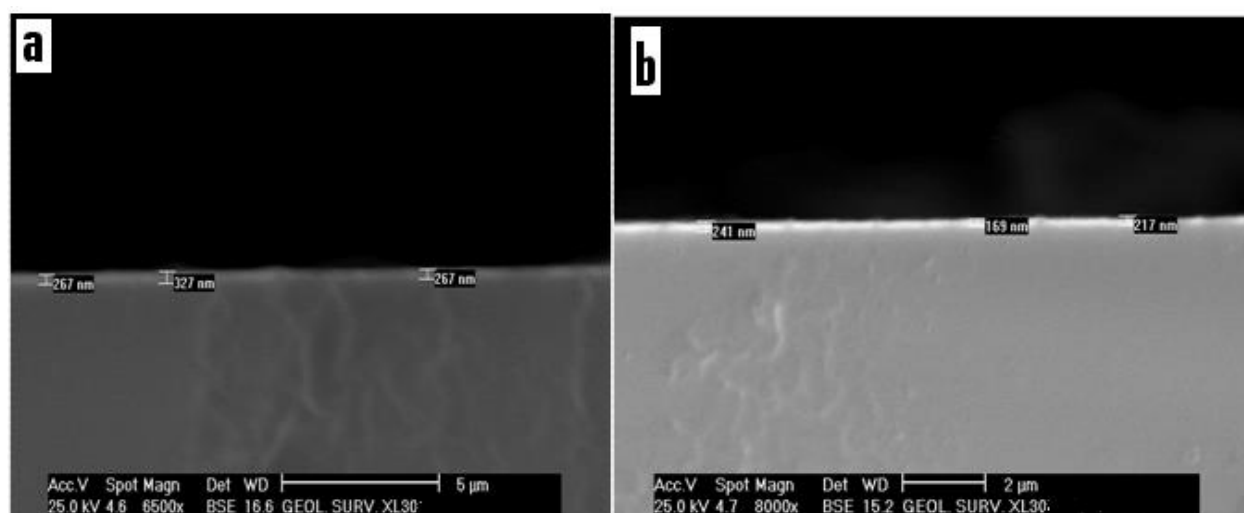
Figure 4: SEM-cross sectional micrographs for films a) dried at 120°C , and b) annealed at 700°C for 2 hours..

Error! Reference source not found. shows scanning electron microscope photographs of all films. From figure 3-a one can see that the dried film at 120°C is amorphous in coincidence with the XRD pattern. Agglomerates start to appear at 300°C with size about 500 nm. The density of agglomerates increases as the annealing temperature increase to 500°C as shown in **Error! Reference source not found.**. Finally at 700°C annealing temperature agglomerates size about 375nm is recorded.

## 3.3 Thickness measurement

The thickness of dried and annealed films has been measured using cross section SEM micrograph. **Error! Reference source not found.** shows the obtained micrographs of the dried film and that annealed at 700°C. As observed the thickness of the film decrease from 287 nm of dried film to 208 nm for sample annealed at 700°C. Such reduction in the films thickness could be attributed to the increase in the film density upon annealing. Thickness variation is observed in all films as a result of the precursor nature of the as deposited films. The thickness of all films was taken as the average over all recorded values, see table 1.

3.4 Optical band gap.

The nature of the optical transition has been investigated using Tacu's relation for direct allowed transition;

$$\alpha h v = \alpha_o (h v - E_g)^{1/2} \qquad (1)$$
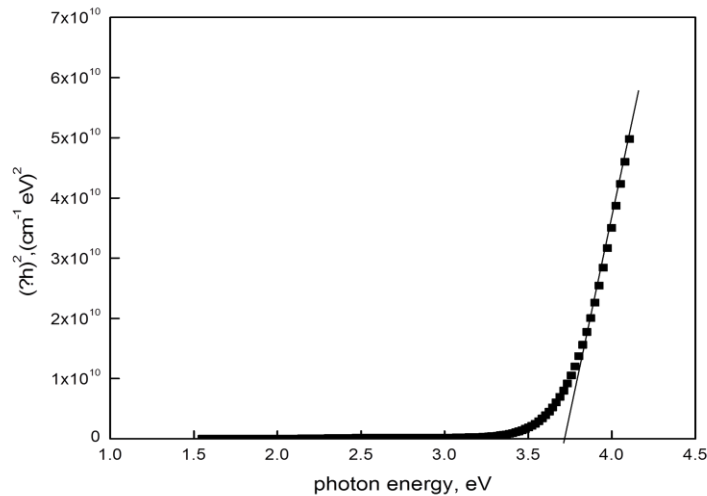
Figure 5:- Absorption coefficient plotted as (αhν)^2 vs. (hν) for the film dried at 120°C.

where $h\nu$ is the photon energy, E_g is the band gap energy and α_o is a constant nearly independent of the photon energy. Figure 5 shown the $(\alpha h\nu)^2$ versus (hv) for the as deposited sample dried at 120°C. A straight line is observed in photon energy region > 3.5 eV in good matching with equation (1). By extrapolating this straight line to meet zero $(\alpha h\nu)^2$ point, the optical band gap can be determined. Table 1 lists the band gap values for all films where no changes in the optical bang gap values up to annealing at 500°C. But at 700°C a significant reduction in the band gap has been recorded. Such reduction in the optical band gap upon annealing has been observed in the work of Gabrusenoks et al (12) who found 0.5-0.7 difference in the absorption of the optical band gap between amorphous and crystalline WO_3 films.

Akram et al. (13) found that E_g = 3.26 eV for sputtered amorphous WO_3 films and 2.90 eV for sputtered crystalline WO_3 films. Also Deb (14) has found that the optical absorption edge of WO_3 is lowered by 0.38 eV on going from amorphous to crystalline state. There is a large shift to lower energy side between E_g of the thin film annealed at 500˚C and that annealed at 700˚C. This may be due to loss of oxygen for the film annealed at 700˚C where the oxygen nonbonding orbitals cause a considerable density of states in the energy gap and indirect optical transitions expected in this case.

Table 1: thickness and energy gaps of WO_3 films

| sample	Thickness(nm)	Energy gap(Eg), eV
120	287	3.72
300	276	3.7
500	235	3.72
700	209	2.95

3.5 Electrical conductivity (σ)

The D.C. electrical conductivity (σ) of WO_3 thin films has been measured as a function of temperature (T) in the range of 450 to 550 K during cooling. Measurements have been carried out using the direct measurement of sheet resistance in presence of air.

Figure 6 presents a typical plot of lnσ versus 1000/T (where T is the absolute temperature in Kelvins) for WO_3 thin films annealed at 300 and 500˚C for 2 hours. The conductivity increases with increasing the temperature showing a characteristic slope depends on the annealing temperature of the thin film. This behavior follows the Arrhenius equation[];

$$\sigma = \sigma_o \exp(-E_a/2kT) \quad (2)$$

where $\sigma = 1/\rho$ (ρ = resistivity) and E_a is the activation energy for electrical conduction and k is Boltzman's constant.

The values of the activation energy (E_a) have been deduced from the slope of the Arrhenius   curves. E_a values are

1.58 and 0.93 eV for the 300 and 500˚C annealed films, respectively. The values of E_a obtained in the present study

lie nearly around the average values obtained by Deb (1.04 eV) (14) in this range of temperature. The discrepancy
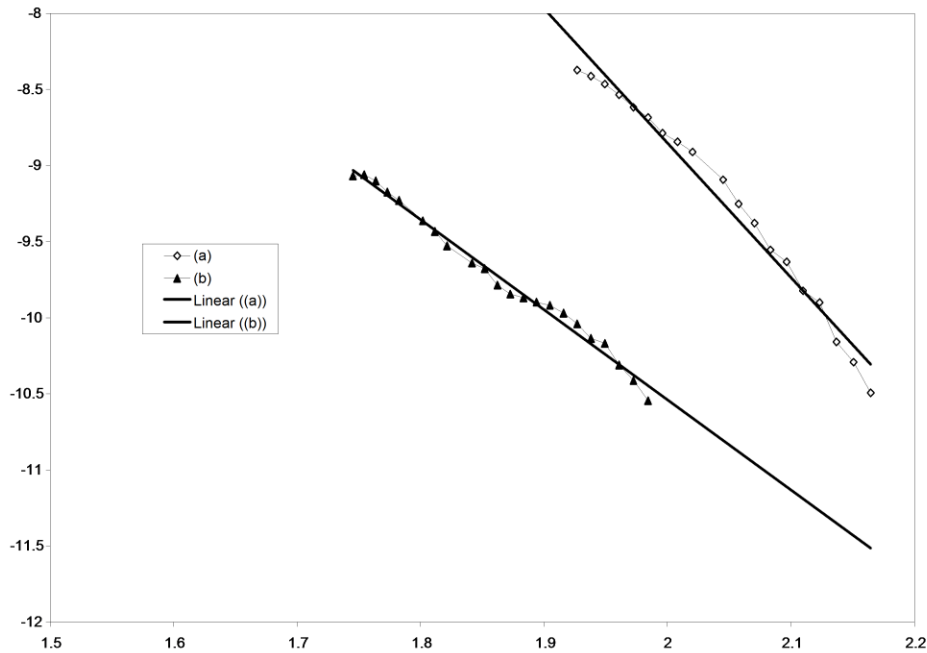
Figure 6: The variation of the ln σ with temperature for WO_3 thin films annealed at a) 300˚C and b)

500˚C.

between our values of E_a and that obtained by Huchins et al.(0.29 eV) (7) and Gillet et al. (0.28 eV) (15) is probably

due to the phase present, crystallinity, the type and concentration of defects and previous thermal history of

specimens used by different authors. WO_3 is considered as n-type semiconductor and we assume that the

nonstoichiometry originates from oxygen vacancies. The creation of oxygen vacancies in WO_3 is followed with two

trapped electrons which give donor states in the energy gap of WO_3. With increasing the temperature of conductivity

measurements, the donors are successfully ionized with an activation of electrons at E_a level, generating free

electrons in the conduction band that increases the conductivity values. In fact, there are many other parameters to

take into account that affect the conductivity values, in particular, the grain size with barriers at grain boundaries and

8

mobility of the carriers. However Gillet et al. (15) have mentioned that WO_3 thin films with different grain sizes exhibit similar conductivity behaviors. In addition, the decrease in the conductivity values of our thin films annealed at 500˚C (crystalline phase) of $E_a = 0.93$ eV with respect to the film annealed at 300˚C (amorphous + crystalline) of $E_a = 1.58$ eV made us believe that the mobility does not play a major role in our specimen. It is more probable that the film of Ea = 0.93 eV has defect concentration content less than that of the film of $E_a = 1.58$ eV in accordance with that reported by Ewald and Kohke (16). They reported that the decrease of the value of the activation energy in semiconductor compounds is accompanied by a decrease in defect concentration content. According to this information, we expect that the thin film annealed at 500˚C has less defect concentration, i.e. more stoichiometric , than that annealed at 300˚C. Therefore we interpret the decrease of the activation energy values of the film annealed at 500˚C due to the crystallinity and stoichiometry.

4. Conclusions

WO_3 thin films have been grown by the Sol-Gel technique followed by an annealing process. Thermal, Structural, microstructure and optical properties, have been studied. The results showed that the as-deposited dried films are amorphous in nature. By increasing the annealing temperature beyond 300^oC the crystalinity of the films starts to increase and peaks start to appear in the x-ray diffraction patterns. In the line of that the optical band gap of the annealed films shows stability at value 3.7eV and decreases to 2.9eV at annealing temperature of 700^oC. The activation energy values (E_a) for electrical conduction of WO_3 thin films deduced from temperature dependence of electrical conductivity measurements, have been found to be depend strongly on the crystallinity and stoichiometry of WO_3 thin film.

References

[1] Granqvist, C. G. Handbook of Inorganic Electrochromic Materials. s.l. : Elsevier .

[2] Avellaneda, C. O. and Bulhões, L. S. Solid State Ionics. 2003, Vol. 165, p. 117.

[3] Naseri, N., et al. International Journal of Hydrogen Energy. 2011, Vol. 36, pp. 13461-13472.

[4] Cotton, F. A. and Wilkinson, G. Advances in Organic Chemistry. s.l. : Wiley, 1988.

[5] Khatko, V., et al. Sensors and Actuators B: Chemical. 2007, Vol. 126, pp. 400-405.

[6] Salinga, C., Weis, H. and Wuttig, M. Thin Solid films. 2002, Vol. 414, p. 275.

[7] Hutchins, M. G., et al. Phys.Stat. Sol.(a). 1999, Vol. 175, p. 991.

[8] Brinker, C. G. and Scherer, G. w. Sol-Gel Sience. San Diego : Academic press, 1990.

[9] N.Özer. Thin Solid Films. 1997, Vol. 304, p. 310.

[10] Ramachandran, R., et al. Ind. J Pure and Appli. Physics. 1999, Vol. 37, p. 353.

[11] 83-0951, JCPDS card No:.

[12] Bertus, L. and Duta, A. Ceramics International. 2012, Vol. 38, pp. 2873-2882.

[13] Akram, H., et al. J. Appl. Phys. 1987, Vol. 62, p. 2039.

[14] Deb, S. K. Phil. Mag. 1973, Vol. 27, p. 801.

[15] Gillet, M., et al. Surf. Sci. 2003, Vols. 532-535, p. 519.

[16] Ewald, A. W. and Kohke, E. E. Phys. Rev. 1955, Vol. 47, p. 607.

[17] Xu, X. Q., Shen, H. and Xiong, X. Y. Thin Soild Films. 2002, Vol. 415, p. 290.

[18] Sun, H. T., et al. Thin Solid Films. 1996, Vol. 287, p. 258.

[19] Lee, D. S., Nam, K. H. and Lee, D. D. Thin Solid Films. 2000, Vol. 375, p. 142.

[20] Giulio, M. Di., et al. J.Phys. D. .

[21] Capone, S., et al. Thin Solid films. 1999, Vol. 350, p. 264.

[22] Regragui, M., et al. Thin Solid films. 2000, Vol. 358 , p. 40.

[23] Regragui, M., et al. Mater. Chemistry and Phys. 2000, Vol. 8915, p. 1.

[24] Naba, T., Nishiyama, Y. and Yasui, I. J. Mater. Res. 1991, Vol. 6, p. 1324.

[25] Varshney, P. K., et al. Indi.J. Pure and Appl. Phys. 1999, Vol. 37, p. 262.

[26] Picquart, M., et al. J.Sol-GelSci. and Tech. 2000, Vol. 18, p. 199.

[27] Sharma, N., et al. J. Non- Cryst. Solid. 2002, Vol. 306, p. 129.

[28] Munro, B., et al. J. Non-Cryst. Solid. 1997, Vol. 218, p. 185.

[29] Damián, M. A., et al. Thin solid films. 2003, Vol. 444, p. 104.